de Melo et al., Irrigat Drainage Sys Eng 2014, 3:3
DOI: 10.4172/2168-9768.1000129

Irrigation & Drainage Systems Engineering

Research Article Open Access

# Impacts of Climate Change on Soybean Irrigation Water Requirements in Northwest Region of Rio Grande do Sul, Brazil

**Tirzah Moreira de Melo*, José Antônio Saldanha Louzada and Olavo Correa Pedrollo**

*Institute of Hydraulic Researches - Federal University of Rio Grande do Sul (IPH/UFRGS), Bento Gonçalves Av, 9500, P.O. Box 15029, Porto Alegre City, State of Rio Grande do Sul, Brazil*

## Abstract

Higher temperatures and a larger variability in precipitation will cause, in general, higher irrigation water requirements. The most important non-irrigated crops for the economy of the state of Rio Grande do Sul, Brazil, are corn and soybeans and the mesoregion which most contributes to the annual harvests of these crops is the Northwest region. This article aims to assess whether the impacts of climate change on agriculture in this region will be positive or negative and in what intensity they may occur. Hence, data from future climate projections generated by different climate models, as well as soil sampling for characterizing physical and hydraulic soil properties were considered. The one-dimensional SWAP model was used to estimate the irrigation water requirements. The results of the hypothesis tests performed for all simulations supports the premise that the irrigation water requirements in the near future (2025s) are not statistically different from the baseline period (1960-1990). On the other hand, water irrigation requirements in 2055s and 2085s reject this hypothesis.

**Keywords:** Future water demands; SWAP model; Climate change impacts; Uncertainty analysis

## Introduction

There is no more doubt that the climate is changing and the Earth is warming, which is mainly attributed to human activities. The current concentration of $CO_2$ in the atmosphere (387 ppm) is higher than it was during the past 800,000 years before the Industrial Revolution, when it ranged from 170 to 280 ppm [1]. This resulted in an increase in average global temperature of 0.74 ± 0.18°C over the last 100 years [2].

Such climate changes are mainly caused by the increase in gas emissions that contribute to the greenhouse effect as a result from human activities, such as burning fossil fuels and deforestation, as well as natural events such as volcanic eruptions [3]. When climate changes occur, all aspects of agriculture should be reviewed, including water demand, irrigation systems, land use, as well as seasonal characteristics of cropping systems [4].

Higher temperatures and a larger temporal variability in precipitation may cause higher water demands for irrigation. This is likely to occur even if the total precipitation during the growing period remains the same [5], and it is mainly due to a higher rate of evapotranspiration.

A recent study [6] indicates that the temperature in Brazil increased by approximately 0.75°C till the end of the past century for all seasons, but more markedly in the period from June to August. It is believed that climate changes subject developing countries, such as Brazil, more vulnerable and that the greatest impacts are likely to be experienced by their ecosystems and agriculture.

In general, with respect to precipitation, it is possible that the rainy season will become wetter, while dry seasons will become even drier. Locations where there is an increase in water deficit for agriculture during the dry months will require much larger quantities of water, intensifying conflicts over its use [7].

To better understand the severity of the consequences, a detailed and careful analysis about the region, the farming practices, the crops and the land uses is of utmost importance. The analysis of historical series of meteorological data allows us to detect local or regional climate patterns and trends over time and space.

During the last decades, the Intergovernmental Panel on Climate Change (IPCC) has summarized the most important researches carried out by the use of several climate models developed around the world. Climate projections are provided by general (GCMs) or regional (RCM) circulation models as a result of future scenarios of climate forcings caused by the emission of greenhouse gases and aerosols. Such models include systems of partial differential equations based on physical laws of fluid motion and chemistry [8], ranging from simple approaches of local energy balance to three-dimensional GCM models (horizontal cell resolution of between 250 and 600 km wide, and 10 to 20 vertical layers in the atmosphere), which attempt to model all complexities of Earth's climate system [9].

Simulation results of different models point to the fact that the effects of climate change on agriculture are also a function of climate scenarios, time slices (for which the uncertainties increase the further we deviate from the baseline period), current local weather and crop management systems and practices [10].

Many authors simulated reductions in crop duration of various crops along this century due to an increase in temperature [4,11,12]. While it had been shown the change rates in rice demands for irrigation fell below 3% in South Korea [13], an increase of 26-32% of annual demands for irrigation in California due to a warmer and drier climate was also reported [14], especially at the end of the century. As noted, these results are a function of increasing temperatures and different precipitation regimes predicted at each location.

***Corresponding author:** Tirzah Moreira de Melo, Institute of Hydraulic Researches - Federal University of Rio Grande do Sul (IPH/UFRGS), Bento Gonçalves Av., 9500, P.O. Box 15029, Porto Alegre City, State of Rio Grande do Sul, Brazil, Tel: 55 53 30255894; Fax: 55 51 33087291; E-mail: tirzahmelo@hotmail.com

**Received** September 23, 2014; **Accepted** December 03, 2014; **Published** December 05, 2014

**Citation:** de Melo TM, Louzada JAS, Pedrollo OC (2014) Impacts of Climate Change on Soybean Irrigation Water Requirements in Northwest Region of Rio Grande do Sul, Brazil. Irrigat Drainage Sys Eng 3: 129. doi:10.4172/2168-9768.1000129

The study presented by [6] considered six GCMs projections for Brazil and the scenarios A2 and B2. They have shown an increase in temperature of up to 4°C in 2085s, while larger differences are likely to be experienced from June to October, i.e., winters will become warmer in comparison with the anomalies expected for the summers.

Specifically in the state of Rio Grande do Sul, the accumulated losses of soybean due to long drought periods were registered during summer months, because the crop development coincides with the period of frequent droughts, i.e., from November to March.

The most important non-irrigated crops of the state of Rio Grande do Sul are corn and soybeans and the mesoregion which most contributes to the annual harvests of these crops is the Northwest region. The corn and soybean planted area are 610,442 and 2,747,600 ha, respectively [15]. A serious aggravating factor in this region that justifies conducting this research is the fact that the cropping system is essentially non-irrigated.

Although knowledge about the causes of global warming and its unquestionable consequences are well known, it is extremely complex to define the uncertainties on future projections. Firstly, it is crucial that the model used to simulate the crop development can accurately estimate historical changes in water demands, before simulating the impacts of climate change [16]. Secondly, there is no consensus on how closely the climate models are to represent the uncertainties associated with the generation of meteorological data for future scenarios. Uncertainties inherent in such models can be attributed to different discretizations, parameterizations and carbon cycle models [8,17] also add that the initial conditions and limitations of the models, as well as the forcings that define different scenarios, are potential uncertainties, but known.

Considering the abovementioned aspects of climate change and some of its most significant consequences on agriculture, this article aims to assess whether the impacts of climate change on agriculture predicted for the Northwest region of Rio Grande do Sul will be positive or negative and in what intensity they may occur. Hence, data from future climate projections generated by different climate models (A1B scenario), as well as soil sampling conducted in the area for spatial characterization of the physical and hydraulic soil properties were considered. This evaluation was carried out by using the SWAP model to determine future irrigation requirements. Since this is a relevant variable, an uncertainty analysis was conduct in other to investigate how different the results are and how these differences are likely to contribute to decision-making in the future.

## Materials and Methods

### Study area

The study area is located in Pejuçara city, Northwest region of the state of Rio Grande do Sul and comprises the Donato basin, with an area of 1.10 km² (Figure 1). The mean of maximum temperatures in

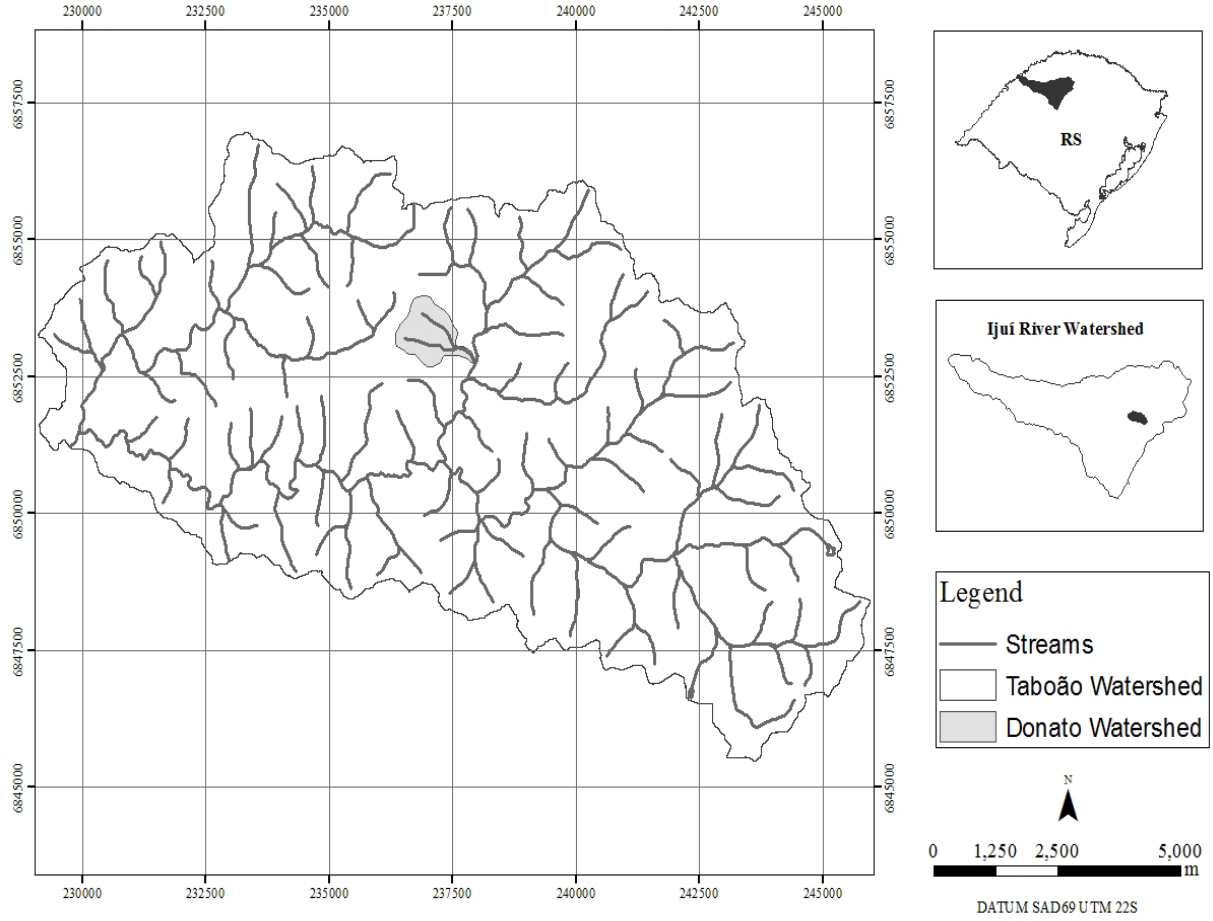


**Figure 1:** Donato basin location.

this region is above 22ºC and the minimum temperature oscillates between -3 and 18ºC. The average (1990-2001) annual rainfall is 1826 mm, October being the wettest month (216 mm) and August the driest (84 mm). The mean relative humidity is 74%, approximately [18]. The soils of the basin have high percentages of clay (> 60%), classified as Dystric Latosols and Eutric Nitosols**.**

The land use is primarily agricultural with the practice of no-till farming in the entire basin. Wheat, oats and soybeans are the most common crops cultivated. Soybean is sown in the summer and wheat or oats during the winter, all non-irrigated. From 1991 to 2012, soybean yields increased eight times and this is the tendency for the future [15]. The crops, soils and its use are representative of the northwest region of Rio Grande do Sul.

## SWAP model

This one-dimensional model simulates the water and heat flow, solute transport, crop development and its interaction with surface water, based on the concepts and current techniques of modeling and simulation [19].

The water balance in the soil profile is the reference for all other modules, obtained by numerical solution of the nonlinear Richards equation [20]. In the SWAP model this equation has the general form:

$$\frac{\partial \theta}{\partial t} = \frac{\partial}{\partial z}\left[k(\theta)\left(\frac{\partial h}{\partial z} + 1\right)\right] - S_a(h) - S_d(h) - S_m(h) \quad (1)$$

where θ is the volumetric water content ($cm^3\ cm^{-3}$), z is depth along the soil profile (cm), k(θ) is the unsaturated hydraulic conductivity (cm $d^{-1}$), h is the soil pressure head (cm ), t is time (d), $S_a(h)$ corresponds to the soil water extraction rate by plant roots ($cm^3\ cm^{-3}\ d^{-1}$), $S_d(h)$ represents the extraction rate by drain discharge in the saturated zone ($d^{-1}$) and $S_m(h)$ is the exchange rate of water between the soil matrix and macro pores ($d^{-1}$).

The numerical discretization of Richards equation is carried out using an implicit finite difference scheme, such that it allows the simultaneous simulation of the saturated and unsaturated zones. The SWAP model solves Equation (1) using known relationships between θ, h and K according to the combination of [21] and [22] models.

## Soil samples

The SWAP model requires input on some soil physical and hydraulic properties such as the saturated hydraulic conductivity and the soil water retention curve. Thus, 55 points in the Donato basin were chosen, dispersed in a regular grid of approximately 140×140 m, with the most distant samples separated 200 m.

In each point, 4 samples were collected; two at 30 cm and two at 60 cm depth. For each depth, one sample was used to determine the soil water retention curve (RC) at pressures of 0.1, 0.3, 0.5, 0.7, 1.0, 1.5, 2.0, 2.5, 3.0 and 5.0 atm using the Richards chamber method. It was assumed that this pressure limit was sufficient to characterize the plant roots zone, since the first soil sample collected provided almost horizontal retention curves. The other sample was used to determine the saturated hydraulic conductivity ($K_{sat}$), obtained experimentally by the variable head permeameter method.

For each retention curve, the parameters of the model of [23] were adjusted according to Equation (2) and using the RETC software [23]. As some adjusted values of α were very large compared to the others, it was preferred to calculate the median of each of the parameters in the retention curve instead of the average, since the latter would be affected by extreme values. In the case of $K_{sat}$, the averages at 30 and 60 cm were considered.

$$\theta(h) = \theta_{res} + (\theta_{sat} - \theta_{res})(1 + |\alpha h|^n)^{-m} \quad (2)$$

where $\theta_{sat}$ is the saturated water content ($cm^3\ cm^{-3}$), $\theta_{res}$ is the residual water content in the very dry range ($cm^3\ cm^{-3}$) and α ($cm^{-1}$), *n* (-) and *m* (-) are empirical shape factors, with m = 1- (1/n). The final parameters used to characterize the physical and hydraulic properties of the soil are presented in Table 1.

## Meteorological data

The SWAP model also requires input on a set of meteorological information concerning the daily time series of the variables: precipitation (P-mm), air vapor pressure (U-kPa), minimum and maximum temperatures (Tmin and Tmax-°C), wind speed (V-m/s) and solar radiation (R-KJ/$m^2$). These variables were used to calculate the reference evapotranspiration ($ET_{ref}$).

In order to use meteorological data that were representative of the study area, climate projections from 7 different locations in the vicinity of the basin were considered (Figure 2), described in Table 2 and divided into the baseline (1961-1990), near term (2011-2040, 2025s), midterm (2041-2070, 2055s) and far term (2071-2100, 2085s). The GCMs considered are shown in Table 3, for which only monthly series of meteorological data in each location were initially available.

Besides these GCMs models, projections generated by the regional ETA model were also applied. This model is a descendant of the HIBU (Hydrometeorological Institute and Belgrade University) model, previously developed by [24]. It is a regional model that couples the HadCM3 general circulation model as lateral boundary condition for mesoscale simulations. A more detailed description of this method can be found in [25]. The coupling of this global model considers a set of regional members (CTRL, LOW, MID and HIGH), representing the climate sensitivity. The horizontal resolutions were 20 and 40 km, then providing 5 other projections: ETA 20-CTRL, ETA 40-CTRL, ETA 40-LOW, ETA 40-MID, ETA-40 HIGH. Yet, only the control member of each GCM was considered and hereafter they will be mention simply by their abbreviations, as shown in Table 3.

The daily series of meteorological data for GCMs were then generated by the Change Factor method [26]. This method of bias correction is based on the calculation of anomalies between the values predicted by climate models in the baseline and future time slices. The anomaly is then used to perturb the observed series of the variable in the baseline period generating the corrected series to be used in future periods. In this work, the time series to be disturbed were obtained after bias correction of the control member (CTRL) of the ETA-40 model. Thus, all the results generated by the use of global models should be compared with the baseline period related to the ETA 40-CTRL model.

Thus, for each of the 7 locations shown in Table 2, there are 10 sets

| Parameter | Soil depths | |
|---|---|---|
| | 30 cm | 60 cm |
| Hydraulic conductivity, $K_{sat}$ (cm/d) | 25.4549 | 12.416 |
| Parameter α ($cm^{-1}$) | 0.1276 | 0.5046 |
| Residual water content, $\theta_{res}$ ($cm^3\ cm^{-3}$) | 0.0000 | 0.0000 |
| Saturated water content, $\theta_{sat}$ ($cm^3\ cm^{-3}$) | 0.4940 | 0.5088 |
| Parameter n (-) | 1.0652 | 1.0407 |

**Table 1:** Fitted soil water retention curve parameters.

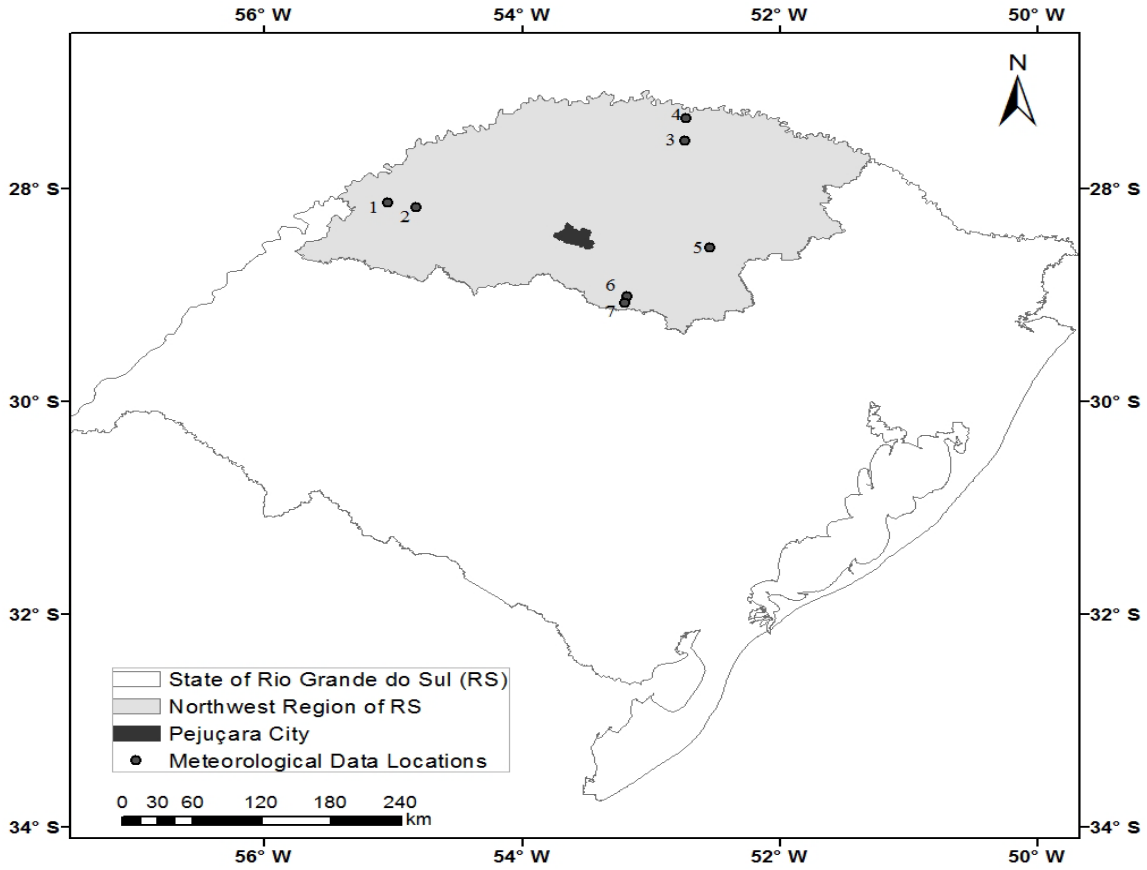


**Figure 2:** Locations of meteorological data.

| Location | City | Latitude (°) | Longitude (°) | River | Altitude (m) |
|---|---|---|---|---|---|
| 1 | Roque Gonzales | -28.14 | 55.05 | Ijuí | 123 |
| 2 | Salvador das Missões | -28.18 | 54.83 | Ijuí | 138 |
| 3 | Entre Rios do Sul | -27.55 | 52.74 | Passo Fundo | 590 |
| 4 | Nonoai/Faxinalzinho | -27.35 | 52.73 | Passo Fundo | 275 |
| 5 | Tio Hugo | -28.56 | 52.55 | Jacuí | 470 |
| 6 | Salto do Jacuí | -29.02 | 53.19 | Jacuí | 323 |
| 7 | Salto do Jacuí | -29.07 | 53.21 | Jacuí | 283 |

**Table 2:** Meteorological data locations in Northwest region of Rio Grande do Sul.

| Model | Abbreviation* | Modeling group |
|---|---|---|
| CCSM3, 2005 | NCCCSM | National Center for Atmospheric Research, USA |
| ECHAM5/MPI-OM, 2005 | MPEH5 | Max Planck Institute for Meteorology, Germany |
| GFDL-CM2.1, 2005 | GFCM21 | U.S Dept. of Commerce/NOAAA/Geophysical Fluid Dynamics Laboratory, USA |
| MRI-CGCM2.3.2, 2003 | MRCGCM | National Center for Atmospheric Research, USA |
| UKMO-HadCM3, 1997 | HADCM3 | Hadley Centre for Climate Prediction and Research/Met Office, United Kingdom |

*Abbreviation adopt in this study.

**Table 3:** General circulation models applied in this study.

of meteorological data derived from these different models. All sets of data will be used in the uncertainty analysis of the climate variables.

## Modelling process

The general form of the Richards equation (Eq. 1), when applied by SWAP model to achieve the objectives of this study, becomes:

$$\frac{\partial \theta}{\partial t} = \frac{\partial}{\partial z}\left[k(\theta)\left(\frac{\partial h}{\partial z} + 1\right)\right] - S_a(h) \quad (3)$$

where only the term of water extraction by plant roots ($S_a(h)$) will be considered and it is assumed that this term is equal to the crop transpiration. The crops at Donato basin are non-irrigated. When calculating future irrigation demands it will be assumed that the total water requirement of the crop will be supplied, and therefore:

$$IWR = T_p - T_a \quad (4)$$

where IWR is the irrigation water requirement (cm), $T_p$ is the

potential transpiration (cm) when the plant has no water limitation and $T_a$ is the actual transpiration (cm). Thus, any value lower than the potential transpiration means that the crop will suffer a water deficit and will need to be irrigated. The IWRs were evaluated for soybean only, since this is the most important crop in the region for which irrigation could be profitable. This is justified by the fact that in 2012 soybean production in this region was 3,585,710 tons compared to only 1,731,219 tons of corn. Additionally, soybean cultivated area (ha) is almost five times greater than for corn [15].

A different simulation for each of the ten climate projections and each of the seven data sources was performed, totaling 70 simulations (Figure 3 for methodology scheme illustration). Initially, the SWAP model calculates the evapotranspiration for a hypothetical reference crop based on the Penman-Monteith equation (not shown), assuming the crop height of 0.12 m, a fixed surface resistance of 70 s $m^{-1}$ and an albedo of 0.23, as bellow:

$$ET_{ref} = \frac{0.408\Delta(R_n - G) + \gamma \frac{900}{T+273} u_2 (e_s - e_a)}{\Delta + \gamma(1 + 0.34u_2)} \quad (5)$$

where $ET_{ref}$ is the transpiration rate of the canopy (mm $day^{-1}$), Δ is the slope vapour pressure curve (kPa $°C^{-1}$), $R_n$ is the net radiation flux at the canopy surface (J $m^{-2}$ $day^{-1}$), G is the soil heat flux density (MJ $m^{-2}$ $day^{-1}$), $e_s$ is the saturation vapour pressure (kPa), $e_a$ is the actual vapour pressure (kPa), γ is the psychrometric constant (kPa $°C^{-1}$), $u_2$ is the wind speed at 2 m height (m $s^{-1}$) and T is the mean daily air temperature at 2 m height (°C).

From $ET_{ref}$ calculated in the previous step, the model then calculates the evapotranspiration for soybean (ETc) by using the coefficient of culture ($k_c$):

$$ET_c = k_c \cdot ET_{ref} \quad (6)$$

In very dry conditions, the evaporation rate declines much faster than transpiration, and for this reason the SWAP considers the calculation of these rates separately. At this stage, therefore, using the leaf area index (LAI), the model separates the evaluation of the potential transpiration ($T_c$) of a crop and the potential evaporation (Ep) of the soil. Yet, when the crop is wet due to interception, SWAP assumes that the energy available for evapotranspiration is entirely used to evaporate the intercepted water, independent of the soil cover fraction ($W_{frac}$). This is valid for higher values of $W_{frac}$. The potential evaporation is then calculated by:

$$E_p = E_{p0}(1 - W_{frac}) e^{-\kappa_{gr} LAI} \quad (7)$$

where $W_{frac}$ (-) is the fraction of the day that the crop is wet, $P_i$ (cm $d^{-1}$) is the ratio of the daily amount of intercepted precipitation, $ET_{w0}$ (cm $d^{-1}$) is the potential evapotranspiration rate for the wet canopy, $E_{p0}$ (cm $d^{-1}$) is the evaporation rate of a wet bare soil and $\kappa_{gr}$ (-) is the extinction coefficient for solar radiation. From equation 7, SWAP calculates $T_c$ by the difference:

$$W_{frac} = \frac{P_i}{ET_{w0}} \quad (8)$$

$$T_c = ET_c (1 - W_{frac}) - E_p \quad (9)$$

where $ET_c$ (cm $d^{-1}$) is the total evapotranspiration rate in periods with dry canopy.

The actual transpiration ($T_a$) is then calculated by taking into account only the water stress due to dry conditions. This is because the critical pressure heads reported for the model will force conditions in which the crop will not suffer a reduction in potential transpiration due to wet conditions, thus preventing it from being incorporated into IWR evaluation. When integrated over the entire depth of the roots, the maximum rate of water uptake by the plant roots (hence, potential) is given by [27]:

$$S_c(z) = \frac{\ell_{root}(z)}{\int_{-D_{root}}^{0} \ell_{root}(z)\, dz} T_c \quad (10)$$

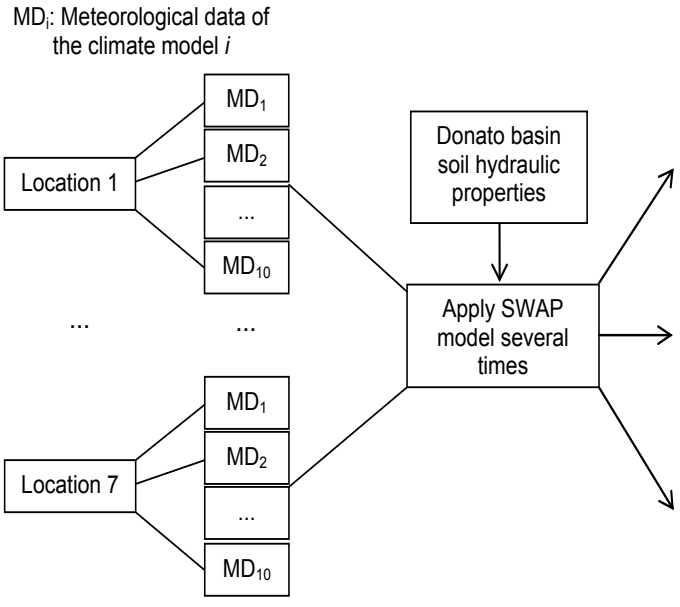


**Figure 3:** Methodology scheme illustration. IWR is the irrigation water requirement of 2025s, 2055s and 2085s time slices.

where $S_c(z)$ is the potential root water extraction rate at a certain depth ($d^{-1}$), $D_{root}$ is the root layer thickness (cm), z is the root depth (cm), $T_c$ is the crop transpiration (cm), $\ell_{root}(z)$ is the root length density distribution.

Thus, water stress of dry conditions will reduce the value of $S_c(z)$ to its actual value $S_a(z)$ by:

$$S_a(z) = \alpha S_c(z) \quad (11)$$

where α is the stress factor of water stress of dry conditions.

Integrating $S_a(z)$ along the root zone, then the crop actual transpiration is given by:

$$T_c = \int_{D_{root}}^{0} S_a(z)dz \quad (12)$$

## Results and Discussions

### Meteorological data

The mean annual temperature (T) and cumulative precipitation (P) for the Northwest region of Rio Grande do Sul during the baseline and future periods are shown in Figure 4. The curves represent the average temperature and precipitation projections considering all 70 (7 locations *versus* 10 climate projections). The baseline period reveals that the temperature has already increased at about 1.71°C while the projections for 2025s indicate an even warmer climate, with an increase of over 3.12°C till the end of the century.

Climate projections also suggest an increase in precipitation, but lesser pronounced than for the temperature. Table 4 presents the average temperature and rainfall projected by GCMs and the RGM. All models predicted a gradual increase in temperature, while the projections of ETA 20 and ETA 40 models provide the strongest increases in precipitation compared to the baseline period.

Figure 5 presents the average annual temperature and precipitation anomalies for all different locations in the study area. The anomalies (Δ) refer to the difference between a variable in a future time slice (for example, 2011-2040) and the same variable in the baseline period (1961-1990). Notice that although the temperature anomalies in some locations are very similar, the same pattern does not repeat for precipitation anomalies, where the variability is much greater. The largest anomalies were predicted for the end of the century, and a reduction in T and P in the short term (2025s) is expected only in location 6. Based on these differences, this study proposes to assess the impact of climate change on future water demands for irrigation, considering these different possibilities for the future climate.

### Irrigation Water Requirement (IWR)

Table 5 presents the average cumulative IWRs (cm) of all simulations obtained with the SWAP model for the baseline, 2025s, 2055s and 2085s periods for each location and climate model. The IWR anomalies are also presented in this table. As global models were generated from daily meteorological data of the ETA 40-CTRL model, IWRs from the formers were compared with the baseline period of this latter (Tables 4 and 5).

As can be seen (Table 5), increasing IWRs are expected for the end of the century (2085s), with the highest values being provided by

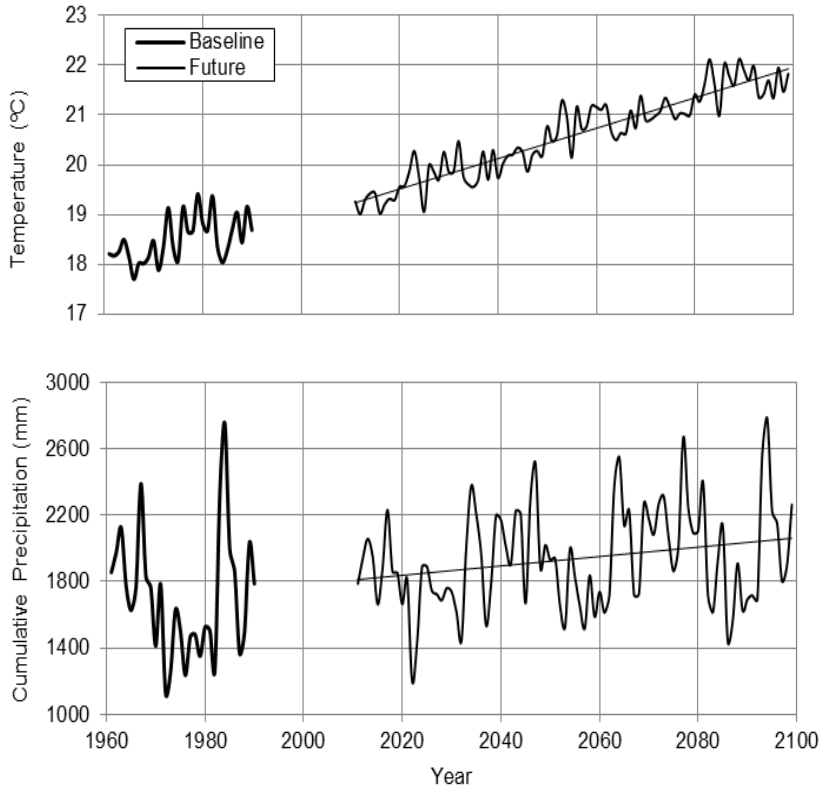


**Figure 4:** Historical and projected average temperature (°C) and average annual cumulative precipitation (mm) of all locations and models. The curves refer to the arithmetic mean of the 70 time series (7 locations and 10 models) of temperature and precipitation.

| Variable | Time Slice | Models | | | | | | | | | |
|---|---|---|---|---|---|---|---|---|---|---|---|
| | | ETA 20 | ETA 40 CTRL | ETA 40 HIGH | ETA 40 LOW | ETA 40 MID | GFCM21 | HADCM3 | MPEH5 | MRCGCM | NRCCCSM |
| Temperature (ºC) | Baseline | 18.98 | | | | | | | | | |
| | 2025s | 19.9 | 19.7 | 20.0 | 19.3 | 20.0 | 19.6 | 19.8 | 19.4 | 19.2 | 19.7 |
| | 2055s | 20.9 | 20.6 | 21.1 | 20.2 | 21.0 | 21.1 | 20.8 | 20.3 | 20.0 | 20.5 |
| | 2085s | 21.2 | 21.3 | 22.5 | 20.6 | 22.1 | 21.7 | 22.2 | 21.6 | 20.3 | 21.0 |
| Cumulative Precipitation (mm) | Baseline | 1724.9 | | | | | | | | | |
| | 2025s | 1953.7 | 1904.8 | 1840.3 | 1923.0 | 1995.5 | 1685.8 | 1701.4 | 1720.5 | 1785.5 | 1855.8 |
| | 2055s | 2083.9 | 2086.2 | 1989.5 | 2089.8 | 2187.4 | 1429.2 | 1865.4 | 1851.2 | 1987.7 | 1921.8 |
| | 2085s | 2266.5 | 2206.9 | 2151.5 | 2339.5 | 2065.1 | 1426.0 | 1834.2 | 1936.7 | 2093.1 | 1982.4 |

**Table 4:** Average annual temperature and precipitation projected by different climate models.

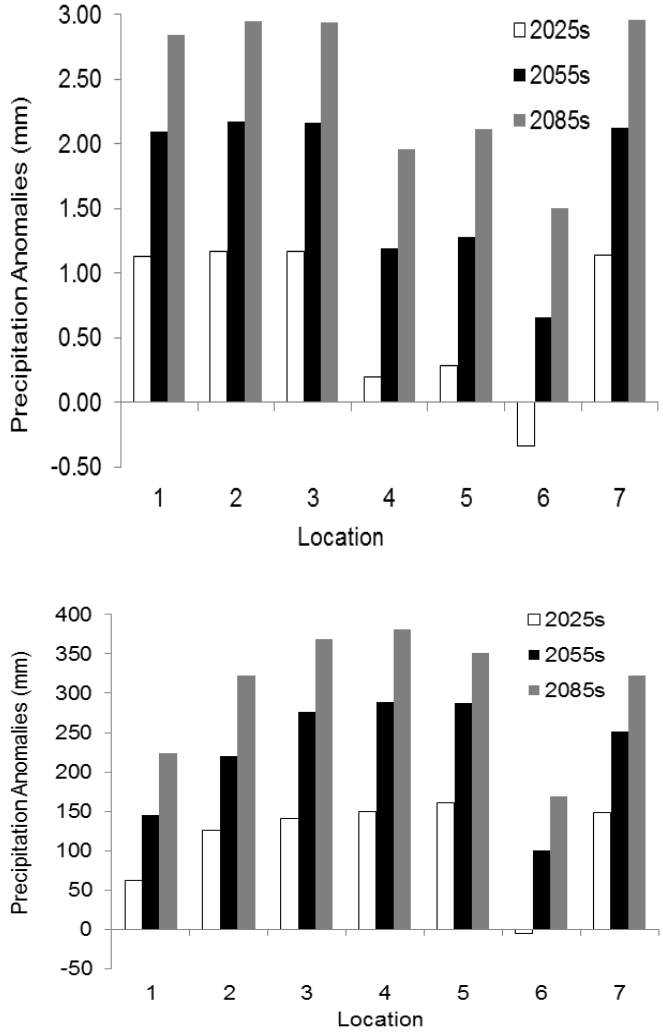


**Figure 5:** Anomalies in average temperature and precipitation for different time slices and locations.

global models. Notice also the differences among the locations, which demonstrated the degree of uncertainty of IWR forecasted for the region. In most cases, ETA model projections indicate a reduction in IWR, while global models suggest the opposite, except for MRCGCM and NRCCCSM models in some locations.

It could be concluded that models do not agree during 2025s, because some of them suggest a reduction in IWRs while others suggest an increasing in IWRs. In 2055s, it is observed that in most locations prevail estimates of reductions, probably due to a higher cumulative precipitation, and this is the period when the models agree more often. Similar behavior can be observed during the end of the century (2085s).

The histograms in Figure 6 correspond to all 70 IWRs calculated for the study area. It is evident that the influences of climate change on water demands for irrigation will be less severe in the short term due to lower data departure around the mean of the baseline period (7.22 cm). In subsequent periods, higher frequencies of IWR simulated above this

| Model | Baseline | IWR (2025s) | IWR (2055s) | IWR (2085s) | Δ˙ (2025s) | Δ (2055s) | Δ (2085s) |
|---|---|---|---|---|---|---|---|
| Location 1 | | | | | | | |
| ETA 20 | 4.11 | 4.91 | 3.32 | 1.32 | 0.80 (19) | -0.79 (-19) | -2.79 (-68) |
| ETA 40 CTRL | 5.13 | 5.11 | 3.20 | 2.14 | -0.02 (0) | -1.93 (-38) | -2.99 (-58) |
| ETA 40 HIGH | 4.83 | 4.15 | 3.79 | 5.14 | -0.68 (-14) | -1.04 (-22) | 0.31 (6) |
| ETA 40 LOW | 5.22 | 3.12 | 2.39 | 2.52 | -2.10 (-40) | -2.83 (-54) | -2.70 (-52) |
| ETA 40 MID | 5.61 | 8.36 | 8.41 | 10.50 | 2.75 (49) | 2.80 (50) | 4.89 (87) |
| GFCM21 | 5.13 | 5.64 | 10.34 | 8.91 | 0.51(10) | 5.21 (102) | 3.78 (74) |
| HADCM3 | 5.13 | 7.63 | 7.77 | 7.57 | 2.50 (49) | 2.64 (51) | 2.44 (48) |
| MPEH5 | 5.13 | 6.49 | 7.90 | 11.67 | 1.36 (27) | 2.77 (54) | 6.54 (127) |
| MRCGCM | 5.13 | 5.43 | 5.30 | 6.13 | 0.30 (6) | 0.17 (3) | 1.00 (19) |
| NRCCCSM | 5.13 | 4.19 | 4.13 | 5.33 | -0.94 (-18) | -1.00 (-19) | 0.20 (4) |
| Location 2 | | | | | | | |
| ETA 20 | 5.28 | 5.05 | 3.48 | 2.01 | -0.23 (4) | -1.80 (-34) | -3.27 (-62) |
| ETA 40 CTRL | 6.10 | 6.56 | 4.29 | 3.69 | 0.46 (8) | -1.81 (-30) | -2.41 (-40) |
| ETA 40 HIGH | 5.98 | 5.38 | 4.72 | 6.11 | -0.60 (-10) | -1.26 (-21) | 0.13 (2) |
| ETA 40 LOW | 6.22 | 4.20 | 3.57 | 2.86 | -2.02 (-32) | -2.65 (-43) | -3.36 (-54) |
| ETA 40 MID | 5.83 | 2.25 | 3.00 | 4.76 | -3.58 (-61) | -2.83 (-49) | -1.07 (-18) |
| GFCM21 | 6.10 | 6.90 | 11.10 | 9.72 | 0.80 (13) | 5.00 (82) | 3.62 (59) |
| HADCM3 | 6.10 | 8.42 | 9.06 | 8.71 | 2.32 (38) | 2.96 (49) | 2.61 (43) |
| MPEH5 | 6.10 | 7.18 | 8.34 | 11.93 | 1.08 (18) | 2.24 (37) | 5.83 (96) |
| MRCGCM | 6.10 | 6.33 | 5.91 | 6.54 | 0.23(4) | -0.19 (-3) | 0.44 (7) |
| NRCCCSM | 6.10 | 5.08 | 5.06 | 6.17 | -1.02 (-17) | -1.04 (-17) | 0.07 (1) |
| Location 3 | | | | | | | |
| ETA 20 | 7.41 | 8.47 | 6.51 | 3.91 | 1.06 (14) | -0.90 (-12) | -3.50 (-47) |
| ETA 40 CTRL | 9.62 | 10.11 | 6.62 | 6.24 | 0.49 (5) | -3.00 (-31) | -3.38 (-35) |
| ETA 40 HIGH | 9.17 | 8.36 | 8.25 | 8.33 | -0.81 (-9) | -0.92 (-10) | -0.84 (-9) |
| ETA 40 LOW | 8.04 | 6.75 | 5.39 | 3.44 | -1.29 (-16) | -2.65 (-33) | -4.60 (-57) |
| ETA 40 MID | 8.74 | 3.93 | 4.59 | 7.12 | -4.81 (-55) | -4.15 (-47) | -1.62 (-19) |
| GFCM21 | 9.62 | 10.96 | 15.71 | 14.64 | 1.34 (14) | 6.09 (63) | 5.02 (52) |
| HADCM3 | 9.62 | 12.99 | 14.32 | 13.82 | 3.37 (35) | 4.70 (49) | 4.20 (44) |
| MPEH5 | 9.62 | 10.61 | 10.94 | 14.75 | 0.99 (10) | 1.32 (14) | 5.13 (53) |
| MRCGCM | 9.62 | 10.13 | 9.42 | 10.54 | 0.51 (5) | -0.20 (-2) | 0.92 (10) |
| NRCCCSM | 9.62 | 7.33 | 7.25 | 9.59 | -2.29 (-24) | -2.37 (-25) | -0.03 (0) |
| Location 4 | | | | | | | |
| ETA 20 | 4.21 | 4.18 | 3.00 | 2.94 | -0.03 (-1) | -1.21 (-29) | -1.27 (-30) |
| ETA 40 CTRL | 7.07 | 7.01 | 4.36 | 4.02 | -0.06 (-1) | -2.71 (-38) | -3.05 (-43) |
| ETA 40 HIGH | 6.75 | 5.90 | 6.17 | 6.13 | -0.85 (-13) | -0.58 (-9) | -0.62 (-9) |
| ETA 40 LOW | 5.44 | 4.46 | 3.33 | 2.09 | -0.98 (-18) | -2.11 (-39) | -3.35 (-62) |
| ETA 40 MID | 6.38 | 2.18 | 3.04 | 5.04 | -4.20 (-66) | -3.34 (-52) | -1.34 (-21) |
| GFCM21 | 7.07 | 8.41 | 12.92 | 12.18 | 1.34 (19) | 5.85 (83) | 5.11 (72) |
| HADCM3 | 7.07 | 10.15 | 11.51 | 10.93 | 3.08 (44) | 4.44 (63) | 3.86 (55) |
| MPEH5 | 7.07 | 8.13 | 8.37 | 12.07 | 1.06 (15) | 1.30 (18) | 5.00 (71) |
| MRCGCM | 7.07 | 7.64 | 7.06 | 8.10 | 0.57 (8) | -0.01 (0) | 1.03 (15) |
| NRCCCSM | 7.07 | 4.89 | 4.84 | 6.91 | -2.18 (-31) | -2.23 (-32) | -0.16 (-2) |
| Location 5 | | | | | | | |
| ETA 20 | 7.63 | 7.27 | 6.27 | 4.35 | -0.36 (-5) | -1.36 (-18) | -3.28 (-43) |
| ETA 40 CTRL | 9.17 | 9.40 | 5.44 | 5.47 | 0.23 (3) | -3.73 (-41) | -3.70 (-40) |
| ETA 40 HIGH | 8.66 | 7.40 | 7.06 | 7.21 | -1.26 (-15) | -1.60 (-18) | -1.45 (-17) |
| ETA 40 LOW | 8.09 | 6.43 | 3.88 | 2.96 | -1.66 (-21) | -4.21 (-52) | -5.13 (-63) |
| ETA 40 MID | 8.46 | 3.59 | 3.81 | 6.28 | -4.87 (-58) | -4.65 (-55) | -2.18 (-26) |
| GFCM21 | 9.17 | 10.08 | 14.83 | 13.37 | 0.91 (10) | 5.66 (62) | 4.20 (46) |
| HADCM3 | 9.17 | 11.70 | 13.17 | 12.64 | 2.53 (28) | 4.00 (44) | 3.47 (38) |
| MPEH5 | 9.17 | 10.19 | 10.62 | 14.36 | 1.02 (11) | 1.45 (16) | 5.19 (57) |
| MRCGCM | 9.17 | 9.55 | 8.50 | 10.02 | 0.38 (4) | -0.67 (-7) | 0.85 (9) |
| NRCCCSM | 9.17 | 6.78 | 6.70 | 8.74 | -2.39 (-26) | -2.47 (-27) | -0.43 (-5) |
| Location 6 | | | | | | | |
| ETA 20 | 6.35 | 6.43 | 5.68 | 5.17 | 0.08 (1) | -0.67 (-11) | -1.18 (-19) |
| ETA 40 CTRL | 7.35 | 13.36 | 9.97 | 10.19 | 6.01 (82) | 2.62 (36) | 2.84 (39) |
| ETA 40 HIGH | 6.89 | 12.93 | 12.13 | 12.91 | 6.04 (88) | 5.24 (76) | 6.02 (87) |
| ETA 40 LOW | 7.17 | 11.25 | 8.99 | 8.07 | 4.08 (57) | 1.82 (25) | 0.90 (13) |

| | | | | | | | |
|---|---|---|---|---|---|---|---|
| ETA 40 MID | 6.87 | 3.16 | 3.15 | 5.88 | -3.71 (-54) | -3.72 (-54) | -0.99 (-14) |
| GFCM21 | 7.35 | 8.23 | 11.93 | 10.07 | 0.88 (12) | 4.58 (62) | 2.72 (37) |
| HADCM3 | 7.35 | 9.35 | 10.85 | 9.70 | 2.00 (27) | 3.50 (48) | 2.35 (32) |
| MPEH5 | 7.35 | 8.35 | 9.52 | 13.11 | 1.00 (14) | 2.17 (30) | 5.76 (78) |
| MRCGCM | 7.35 | 7.85 | 6.99 | 8.39 | 0.50 (7) | -0.36 (-5) | 1.04 (14) |
| NRCCCSM | 7.35 | 5.53 | 5.55 | 6.88 | -1.82 (-25) | -1.80 (-24) | -0.47 (-6) |
| Location 7 | | | | | | | |
| ETA 20 | 7.48 | 6.76 | 5.45 | 4.35 | -0.72 (-10) | -2.03 (-27) | -3.13 (-42) |
| ETA 40 CTRL | 7.93 | 8.48 | 4.99 | 4.57 | 0.55 (7) | -2.94 (-37) | -3.36 (-42) |
| ETA 40 HIGH | 7.95 | 6.90 | 6.25 | 7.52 | -1.05 (-13) | -1.7 (-21) | -0.43 (-5) |
| ETA 40 LOW | 8.41 | 6.18 | 3.83 | 2.54 | -2.23 (-27) | -4.58 (-54) | -5.87 (-70) |
| ETA 40 MID | 7.75 | 3.25 | 3.33 | 5.89 | -4.5 (-58) | -4.42 (-57) | -1.86 (-24) |
| GFCM21 | 7.93 | 8.82 | 12.95 | 11.11 | 0.89 (11) | 5.02 (63) | 3.18 (40) |
| HADCM3 | 7.93 | 10.22 | 11.45 | 10.66 | 2.29 (29) | 3.52 (44) | 2.73 (34) |
| MPEH5 | 7.93 | 9.14 | 10.74 | 14.86 | 1.21 (15) | 2.81 (35) | 6.93 (87) |
| MRCGCM | 7.93 | 8.55 | 7.52 | 9.18 | 0.62 (8) | -0.41 (-5) | 1.25 (16) |
| NRCCCSM | 7.93 | 6.08 | 5.99 | 7.46 | -1.85 (-23) | -1.94 (-24) | -0.47 (-6) |

* Δ: irrigation water requirement anomalies (cm); terms in parenthesis indicate percentage change from baseline period.

**Table 5:** Irrigation water requirements (IWRs) and anomalies (Δ) of all simulations and time slices (cm).

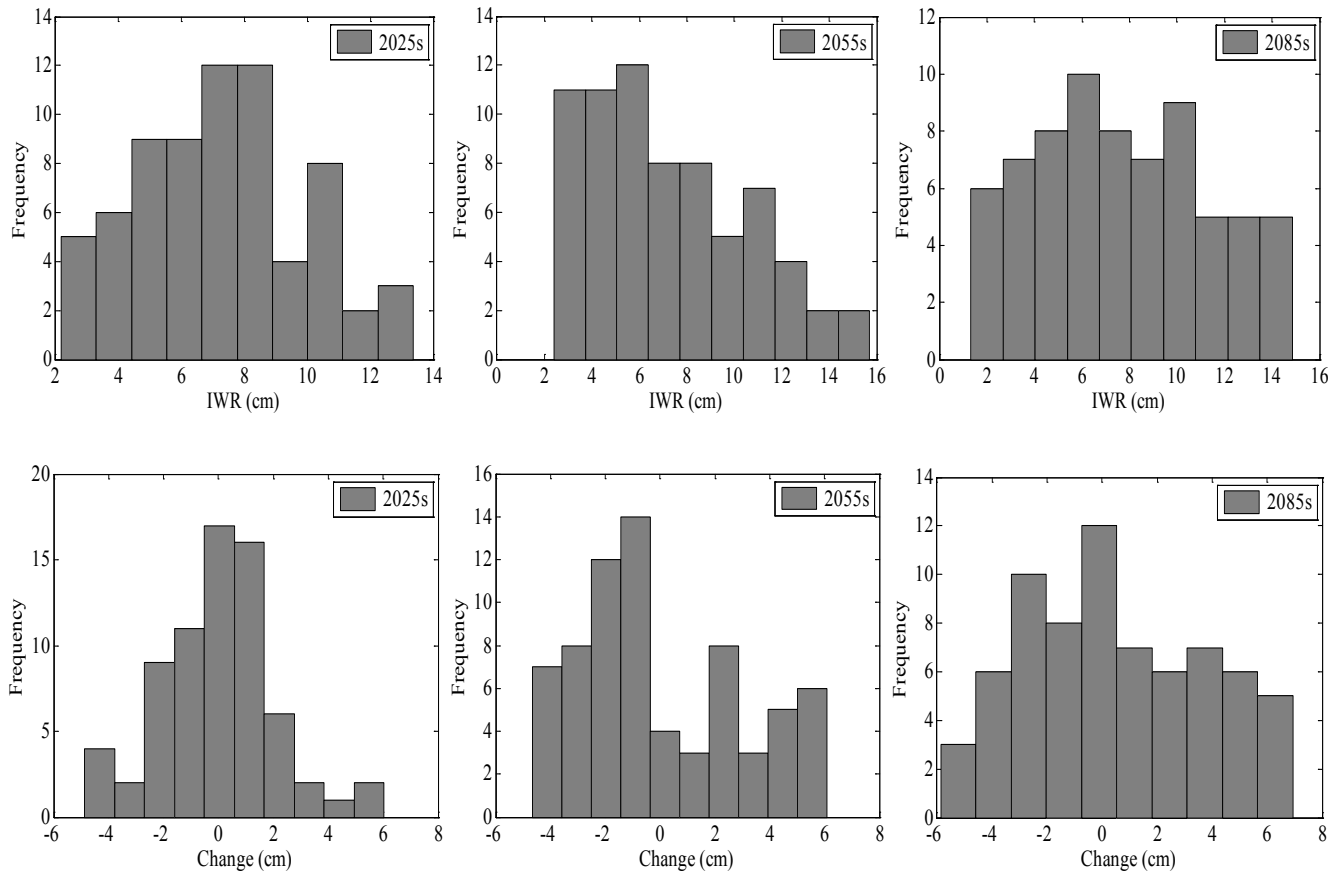


**Figure 6:** Irrigation water requirements and anomalies histograms for all simulations and time slices.

average were obtained. However, the most frequent values are in the range below 7.22 cm, confirming the possibility that the area will be positively influenced by lower irrigation requirements in the future.

Likewise, the analysis of the histograms of the anomalies also confirms that in the short term most of simulations fall on the range around zero, indicating little or no difference with respect to the baseline period. During 2055s, there is a higher frequency of negative anomalies ranging from -4 to -1 cm. Yet, lower frequencies of null or positive anomalies were obtained.

These histograms can also be used to analyse the IWR uncertainties in terms of its anomalies. As expected, the uncertainty during 2085s is higher and is reflected by a more dispersed histogram. These results

are in agreement with predictions of a population growth peak in the middle of the century and the intensification of negative effects on the Earth, such as an increase in temperature and increase or decrease in precipitation amounts.

In order to quantify the uncertainties of the simulations, the IWR cumulative distributions functions (cdfs) were plotted in Figure 7. Table 6 presents the respective percentiles for each of the cdfs to support in the interpretation of the graphs.

Table 6 shows the degree of uncertainty of the simulations. The uncertainties reflect how different all IWRs are, as a result of the use of different meteorological data in SWAP model. This evaluation was carried out for IRW and its anomalies separately. If we take the values between the percentiles of 5 and 95%, we may note that 90% of IWR simulations are between the ranges of 3.16-11.70, 3.04-13.17 and 2.14-14.36 cm, resulting in uncertainties of 8.54, 10.13 and 12.22 cm for 2025s, 2055s and 2085s, respectively. These values are significantly large, demonstrating the error that can be committed when defining which data will be used by the model.

Thus, it is essential that agricultural planning decisions that are based on climate projections should consider the greater number of possible models. For example, according to the projections employed in this study, it can be stated that in 90% of the simulations the average annual IWRs will not be greater than 10.42, 12.03 and 13.01 cm for the three future periods. However, many other forecasts were not included in this analysis, which could add more information about the uncertainties of climate models, or even the future will not match any of them. Only for an average analysis (50% percentile), the future periods are not different from baseline period.

It is worth mentioning that the uncertainties derived from model parameters, among many other sources, were not considered in this study. In addition, these results represent one-dimensional simulations. When the area dimension is considered, the volumes of demanded water will reflect the impacts on water resources.

## Hypothesis test

Although Table 5 presents the anomalies of future water demands compared to the period of 1961-1990, it does not reveal whether each future period is different from the baseline, since they refer to averages of 30 years period. Thus, the two-sample hypothesis test of Kolmogorov-Smirnov was performed to verify whether the probability distribution functions of future IWR were statistically different from the baseline period in each location. In this case, the null hypothesis $H_o$ tests whether the compared cdfs are statistically equal. The results are shown in Table 7 for the significance level $\alpha$=0.05.

Analyzing the values of h in this table, it can be seen that the vast majority of models agree that there are no significant differences between 2025s and the baseline IWRs, except for ETA 40 MID model, which rejects the null hypothesis (h=1) in all locations. During 2055s, the predictions generated by other models also indicate that this period is different from the baseline. The same is observed for the end of the century (2085s), coupled with some other rejections of the null hypothesis.

In general, one can say that there is not enough statistical evidence in most cases to admit that the cdfs differ to the period of comparison for the adopt level of significance. This fact is also reflected by the very high p-value, indicating that it is not safe to reject the null hypothesis without assuming a large error. Greater tendency to reject $H_o$ was observed by simulations performed by ETA model.

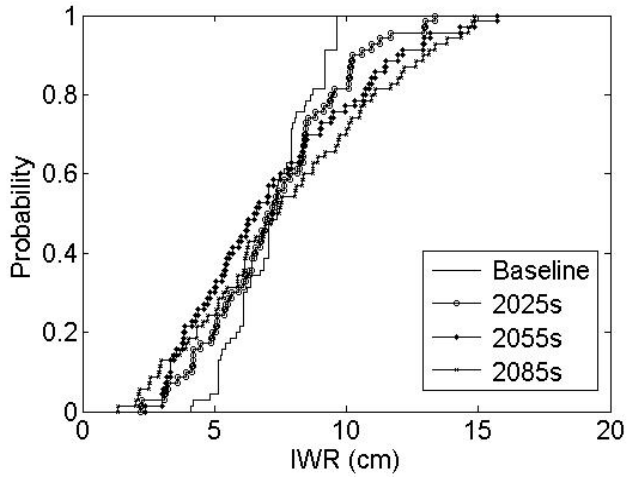


**Figure 7:** Irrigation water requirements and anomalies cumulative distribution functions.

| Percentile | IWR (2025s) | IWR (2055s) | IWR (2085s) | Δ (2025s) | Δ (2055s) | Δ (2085s) |
|---|---|---|---|---|---|---|
| 5 | 3.16 | 3.04 | 2.14 | -4.20 | -4.21 | -3.70 |
| 25 | 5.38 | 4.36 | 4.76 | -1.05 | -2.23 | -2.41 |
| 50 | 7.10 | 6.57 | 7.34 | 0.34 | -0.85 | 0.10 |
| 75 | 8.82 | 9.52 | 10.50 | 1.06 | 2.64 | 3.18 |
| 90 | 10.42 | 12.03 | 13.01 | 2.52 | 4.85 | 5.12 |
| 95 | 11.70 | 13.17 | 14.36 | 3.37 | 5.24 | 5.83 |

**Table 6:** Cumulative distribution functions percentiles of irrigation water requirements and anomalies (cm).

| | ETA 20 | ETA 40 CTRL | ETA 40 HIGH | ETA 40 LOW | ETA 40 MID | GFCM21 | HADCM3 | MPEH5 | MRCGCM | NRCCCSM |
|---|---|---|---|---|---|---|---|---|---|---|
| Location 1 | | | | | | | | | | |
| h[a] (2025s) | 0 | 0 | 0 | 0 | 1 | 0 | 0 | 0 | 0 | 0 |
| p[b] | 0.9360 | 0.9360 | 0.3420 | 0.1088 | 0.0017 | 0.9360 | 0.1088 | 0.5372 | 0.9970 | 0.5372 |
| D[c] | 0.1333 | 0.1333 | 0.2333 | 0.3000 | 0.4667 | 0.1333 | 0.3000 | 0.2000 | 0.1000 | 0.2000 |
| h (2055s) | 0 | 0 | 0 | 0 | 1 | 1 | 0 | 0 | 0 | 0 |
| p | 0.2003 | 0.2003 | 0.5372 | 0.0550 | 0.0006 | 0.0113 | 0.0550 | 0.1088 | 0.9970 | 0.3420 |
| D | 0.2667 | 0.2667 | 0.2000 | 0.3333 | 0.5000 | 0.4000 | 0.3333 | 0.3000 | 0.1000 | 0.2333 |
| h (2085s) | 1 | 1 | 0 | 0 | 1 | 1 | 0 | 1 | 0 | 0 |
| p | 0.0010 | 0.0022 | 0.8383 | 0.0627 | 0.0008 | 0.0325 | 0.2468 | 0.0026 | 0.7240 | 0.9950 |
| D | 0.4897 | 0.4621 | 0.1552 | 0.3299 | 0.4977 | 0.3598 | 0.2563 | 0.4575 | 0.1736 | 0.1046 |
| Location 2 | | | | | | | | | | |
| h (2025s) | 0 | 0 | 0 | 1 | 1 | 0 | 0 | 0 | 0 | 0 |
| p | 0.3420 | 0.9360 | 0.5372 | 0.0259 | 0.0046 | 0.7600 | 0.2003 | 0.7600 | 0.9970 | 0.9360 |
| D | 0.2333 | 0.1333 | 0.2000 | 0.3667 | 0.4333 | 0.1667 | 0.2667 | 0.1667 | 0.1000 | 0.1333 |
| h (2055s) | 1 | 0 | 0 | 1 | 1 | 1 | 0 | 0 | 0 | 0 |
| p | 0.0113 | 0.3420 | 0.2003 | 0.0259 | 0.0259 | 0.0113 | 0.1088 | 0.2003 | 0.9970 | 0.7600 |
| D | 0.4000 | 0.2333 | 0.2667 | 0.3667 | 0.3667 | 0.4000 | 0.3000 | 0.2667 | 0.1000 | 0.1667 |
| h (2085s) | 1 | 1 | 0 | 1 | 0 | 0 | 0 | 1 | 0 | 0 |
| p | 0.0001 | 0.0134 | 0.9670 | 0.0293 | 0.2657 | 0.2706 | 0.4474 | 0.0076 | 0.9977 | 0.9973 |
| D | 0.5598 | 0.3966 | 0.1241 | 0.3644 | 0.2517 | 0.2506 | 0.2161 | 0.4184 | 0.0989 | 0.1000 |
| Location 3 | | | | | | | | | | |
| h (2025s) | 0 | 0 | 0 | 0 | 1 | 0 | 0 | 0 | 0 | 0 |
| p | 0.7600 | 0.9360 | 0.5372 | 0.3420 | 0.0017 | 0.3420 | 0.0550 | 0.3420 | 0.9360 | 0.1088 |
| D | 0.1667 | 0.1333 | 0.2000 | 0.2333 | 0.4667 | 0.2333 | 0.3333 | 0.2333 | 0.1333 | 0.3000 |
| h (2055s) | 0 | 0 | 0 | 0 | 1 | 1 | 1 | 0 | 0 | 0 |
| p | 0.3420 | 0.0550 | 0.3420 | 0.2003 | 0.0259 | 0.0046 | 0.0113 | 0.2003 | 1.0000 | 0.1088 |
| D | 0.2333 | 0.3333 | 0.2333 | 0.2667 | 0.3667 | 0.4333 | 0.4000 | 0.2667 | 0.0667 | 0.3000 |
| h (2085s) | 1 | 1 | 0 | 1 | 0 | 1 | 1 | 1 | 0 | 0 |
| p | 0.0027 | 0.0142 | 0.8045 | 0.0008 | 0.4206 | 0.0189 | 0.0444 | 0.0194 | 0.6858 | 0.9999 |
| D | 0.4563 | 0.3943 | 0.1609 | 0.4943 | 0.2207 | 0.3828 | 0.3460 | 0.3816 | 0.1793 | 0.0828 |
| Location 4 | | | | | | | | | | |
| h (2025s) | 0 | 0 | 0 | 0 | 1 | 0 | 0 | 0 | 0 | 0 |
| p | 0.2003 | 0.7600 | 0.3420 | 0.3420 | 0.0001 | 0.3420 | 0.1088 | 0.5372 | 0.7600 | 0.1088 |
| D | 0.2667 | 0.1667 | 0.2333 | 0.2333 | 0.5667 | 0.2333 | 0.3000 | 0.2000 | 0.1667 | 0.3000 |
| h (2055s) | 0 | 0 | 0 | 0 | 1 | 1 | 1 | 0 | 0 | 0 |
| p | 0.1088 | 0.1088 | 0.5372 | 0.2003 | 0.0113 | 0.0046 | 0.0259 | 0.5372 | 1.0000 | 0.1088 |
| D | 0.3000 | 0.3000 | 0.2000 | 0.2667 | 0.4000 | 0.4333 | 0.3667 | 0.2000 | 0.0667 | 0.3000 |
| h (2085s) | 0 | 1 | 0 | 1 | 0 | 1 | 1 | 1 | 0 | 0 |
| p | 0.1356 | 0.0061 | 0.9030 | 0.0142 | 0.5856 | 0.0206 | 0.0422 | 0.0200 | 0.3698 | 0.9934 |
| D | 0.2908 | 0.4264 | 0.1425 | 0.3943 | 0.1943 | 0.3793 | 0.3483 | 0.3805 | 0.2299 | 0.1069 |
| Location 5 | | | | | | | | | | |
| h (2025s) | 0 | 0 | 0 | 0 | 1 | 0 | 0 | 0 | 0 | 0 |
| p | 0.5372 | 0.9360 | 0.2003 | 0.2003 | 0.0006 | 0.9360 | 0.5372 | 0.9360 | 0.9970 | 0.2003 |
| D | 0.2000 | 0.1333 | 0.2667 | 0.2667 | 0.5000 | 0.1333 | 0.2000 | 0.1333 | 0.1000 | 0.2667 |
| h (2055s) | 0 | 1 | 0 | 1 | 1 | 1 | 1 | 0 | 0 | 0 |
| p | 0.3420 | 0.0259 | 0.3420 | 0.0017 | 0.0046 | 0.0046 | 0.0259 | 0.7600 | 0.9360 | 0.1088 |
| D | 0.2333 | 0.3667 | 0.2333 | 0.4667 | 0.4333 | 0.4333 | 0.3667 | 0.1667 | 0.1333 | 0.3000 |
| h (2085s) | 1 | 1 | 0 | 1 | 0 | 0 | 0 | 1 | 0 | 0 |
| p | 0.0009 | 0.0317 | 0.7975 | 0.0020 | 0.0813 | 0.0852 | 0.1603 | 0.0444 | 0.8869 | 0.9810 |
| D | 0.4920 | 0.3609 | 0.1621 | 0.4655 | 0.3172 | 0.3149 | 0.2816 | 0.3460 | 0.1460 | 0.1172 |
| Location 6 | | | | | | | | | | |
| h (2025s) | 0 | 1 | 1 | 1 | 1 | 0 | 0 | 0 | 0 | 0 |
| p | 0.9360 | 0.0046 | 0.0006 | 0.0259 | 0.0017 | 0.9360 | 0.2003 | 0.7600 | 0.9360 | 0.2003 |
| D | 0.1333 | 0.4333 | 0.5000 | 0.3667 | 0.4667 | 0.1333 | 0.2667 | 0.1667 | 0.1333 | 0.2667 |
| h (2055s) | 0 | 1 | 1 | 0 | 1 | 1 | 0 | 0 | 0 | 0 |
| p | 0.3420 | 0.0113 | 0.0002 | 0.0550 | 0.0017 | 0.0259 | 0.0550 | 0.3420 | 0.9970 | 0.3420 |
| D | 0.2333 | 0.4000 | 0.5333 | 0.3333 | 0.4667 | 0.3667 | 0.3333 | 0.2333 | 0.1000 | 0.2333 |
| h (2085s) | 1 | 1 | 1 | 0 | 0 | 0 | 0 | 1 | 0 | 0 |
| p | 0.0010 | 0.0007 | 0.0001 | 0.1141 | 0.2468 | 0.1704 | 0.3947 | 0.0054 | 0.9030 | 0.9977 |
| D | 0.4897 | 0.5000 | 0.5598 | 0.3000 | 0.2563 | 0.2782 | 0.2253 | 0.4310 | 0.1425 | 0.0989 |

| Location 7 | | | | | | | | | | |
|---|---|---|---|---|---|---|---|---|---|---|
| h (2025s) | 0 | 0 | 0 | 0 | 1 | 0 | 0 | 0 | 0 | 0 |
| p | 0.7600 | 0.9360 | 0.5372 | 0.0550 | 0.0017 | 0.7600 | 0.5372 | 0.7600 | 0.9970 | 0.5372 |
| D | 0.1667 | 0.1333 | 0.2000 | 0.3333 | 0.4667 | 0.1667 | 0.2000 | 0.1667 | 0.1000 | 0.2000 |
| h (2055s) | 0 | 0 | 0 | 1 | 1 | 0 | 0 | 0 | 0 | 0 |
| p | 0.2003 | 0.1088 | 0.5372 | 0.0046 | 0.0006 | 0.1088 | 0.2003 | 0.3420 | 0.9970 | 0.5372 |
| D | 0.2667 | 0.3000 | 0.2000 | 0.4333 | 0.5000 | 0.3000 | 0.2667 | 0.2333 | 0.1000 | 0.2000 |
| h (2085s) | 1 | 0 | 0 | 1 | 0 | 0 | 0 | 1 | 0 | 0 |
| p | 0.0174 | 0.0658 | 0.9977 | 0.0002 | 0.2514 | 0.4822 | 0.5780 | 0.0155 | 0.8574 | 0.9790 |
| D | 0.3862 | 0.3276 | 0.0989 | 0.5322 | 0.2552 | 0.2103 | 0.1954 | 0.3908 | 0.1517 | 0.1184 |

[a] h is the test output ($H_o$ = both samples come from the same distribution; h=1, reject $H_o$; h=0, no statistic evidence to reject $H_o$) ; p is the p-value and D is the test statistic.

**Table 7:** Two-sample Kolmogorov-Smirnov test for irrigation water requirements.

From the results shown in Table 7, it can be inferred that the rejection of the null hypothesis only occurred when differences between the cdfs were strongly large. This fact is because the test is quite conservative, since deviations of 20 to 40% from the baseline period were not considered statistically different in most cases.

For example, analyzing the ETA 40-MID model of location 1, we reject the equality of all future periods compared to the baseline, whereas the test does not reject $H_o$ for ETA 40-LOW model, which also showed significant differences from the comparison period (-40, -54 and -52% for 2025s, 2055s and 2085s, respectively). It should be emphasized that the data presented in Table 5 refer to annual averages for periods of 30 years, but reveal nothing about the behavior of the data distribution.

The statistic of the test (D) is the maximum distance between the distributions tested and when compared among future periods it also indicates which of them is more different from the baseline. It is evident from the results in Table 7 that the highest D values were obtained for simulations of the end of the century (2085s), when it is expected greater uncertainty on climate projections and when models differ more strongly.

The individual analysis of the hypothesis test served to reveal the differences generated by each model and location but does not allow general inferences about the region. Thus, the same test was performed for the distributions of all 70 simulations presented in Figure 7. The test revealed that there is not enough statistical evidence to assume that the 2025s period is different from the baseline, but the test rejects $H_o$ for the other two periods with p-values of 0.1065, 0.005 and 0.00073 and D of 0.2000, 0.2857 and 0.3286 for 2025s, 2055s and 2085s, respectively.

## Conclusions

In this study, future irrigation water requirements in the most important agricultural region of Rio Grande do Sul were determined to analyze how climate change could affect agriculture. The use of different projections of meteorological data provided by global and regional models enabled to identify the degree of uncertainty associated with forecasts of water demand.

In general, what can be concluded is that if the predictions of global models are confirmed, the region is likely to be adversely affected, since the simulations with the SWAP model using these projections indicated an increase in irrigation requirements for soybean. On the other hand, regional models are more accurate to the scale of application and spatial resolution, and in this study they showed significant reductions in water demand for agriculture due to an increase in precipitation till the end of the century.

It should be noted that these projections are not able to satisfactorily reproduce the occurrence of extreme events, such as hail, heavy rains, frosts, which are the major causes of crop losses. However, it is possible that changes in climate conditions in the region will make these events more frequent and, therefore, studies such as this serve to support forms of adaptation even in the short term.

Although it cannot be concluded with certainty whether the impacts will be positive or negative when analyzing the models individually, the results of the hypothesis test performed for all simulations supports the premise that the water demand for irrigation in the near future (2025s) are not statistically different from the baseline (1960-1990), but the opposite was observed from the middle of the century on. These results may support water management studies to define the size of reservoirs, based on climate projections. In this study, we can conclude that global climate projections suggest that larger reservoirs will be needed in the future if it is economically possible to attend 100% of the demand. On the other hand, the projections of the regional climate model ETA suggest that smaller reservoirs will be needed, since it projects an increase in precipitation.

It was shown that the uncertainties are large, although many sources have not been considered. In this study, we assumed that cropping patterns are not affected by climate change, as well as agricultural or irrigation expansion scenarios were not considered. Furthermore, a more detailed analysis of the meteorological variables may indicate which of the weather variables influence the most the results.

However, unlike other sectors, agriculture adapts quickly in the face of atypical weather events. This possibility has not been included here, but it is known that the effects of climate change simulated in this work could have been reduced by assumptions such as genetic enhancements, fertilization management techniques and other choices of crops adapted to the new climate.

### Acknowledgements

We are very thankful to the National Council of Scientific and Technological Development (CNPq) for sponsoring this research and acknowledge all anonymous reviewers for their suggestions and improvements in this paper.

### References

1. World Bank (2009) World Development Report 2010: Development and Climate Change. World Bank, Washington.
2. Trenberth K, Jones P (2007) Observations: surface and atmospheric climate change. In: Solomon S, Qin D, Manning M, Chen Z, Marquis M et al. (eds), Climate Change 2007: The Physical Science Basis. Cambridge University Press, Cambridge, UK and New York, USA.
3. Intergovernmental Panel on Climate Change (IPCC) (2007) Climate Change 2007: Synthesis Report. Core Writing Team, Pachauri, R; Reisinger, A. (Eds). Geneva: IPCC.
4. Hwan Y, Yong C, Hyun L, Gyeong O, Koun Y (2013) Climate change impacts

on water storage requirements of an agricultural reservoir considering changes in land use and rice growing season in Korea. Agr Water Manage 117: 43-54.

5. Bates B, Kundzewicz Z, Wu S, Palutikof J (Eds) (2008) Climate Change and Water Technical Paper of the Intergovernmental Panel on climate Change, IPCC Secretariat, Geneva.
6. Hamada E, Gonçalves R, Orsini J, Ghini R (2008) Future climate scenarios for Brazil. In: Ghini R, Hamada E (eds) Climate Changes: impacts on plant diseases in Brasil. Brasília-DF, EMBRAPA Informação Tecnológica.
7. Harmsen E, Niller N, Schlegel N, Gonzalez J (2009) Seasonal climate change impacts on evapotranspiration, precipitation deficit and crop yield in Puerto Rico. Agr Water Manage 96: 1085-1095.
8. Nkomozepi T, Chung S (2012) Assessing the trends and uncertainty of maize net irrigation water requirement estimated from climate change projections for Zimbabwe. Agri Water Manage 111: 60-67.
9. Barry R, Chorley R (2009) Atmosphere, Weather and Climate, ninth ed. Routledge, New York.
10. 10. Islam A, Ahuja L, Garcia L, Ma L, Saseendran A, et al. (2012) Modeling the impacts of climate change on irrigated corn production in the Central Great Plains. Agri Water Manage 110: 94-108.
11. Jalota S, Kaur H, Kaur S, Vashisht B (2013) Impact of climate change scenarios on yield, water and nitrogen-balance and use efficiency of rice-wheat cropping system. Agri Water Manage 116: 29-38.
12. Bocchiola D, Nana E, Soncini A (2013) Impact of climate change scenarios on crop yield and water footprint of maize in the Po valley of Italy. Agr Water Manage 116: 50-61.
13. Yoo S, Choi J, Nam W, Hong E (2012) Analysis of design water requirement of paddy rice using frequency analysis affected by climate change in South Korea. Agri Water Manage 112: 33-42.
14. Mehta V, Haden V, Joyce B, Purkey D, Jackson L (2013) Irrigation demand and supply, given projections of climate and land-use change, in Yolo County, California. Agri Water Manage 117: 70-82.
15. http://dados.fee.tche.br/
16. Daccachea A, Weatherhead E, Stalhamb M, Knox J (2011) Impacts of climate change on irrigated potato production in a humid climate. Agr Forest Meteorol 151: 1641-1653.
17. Stone D, Knutti R (2010) Weather and Climate. In: Fung C, Lopez A, New M. (eds), Modelling the Impact of Climate Change on Water Resources, Willey-Blackwell, Oxford.
18. http://www.inmet.gov.br/portal/
19. Van Dam J (2000) Field scale water flow and solute transport. SWAP model concepts, parameter estimation and case studies. PhD thesis, Wageningen University.
20. Richards L A (1931) Capillary conduction of liquids through porous mediums. J Appl Phys 1: 318-333.
21. Van Genuchten M (1980) A closed-form equation for predicting the hydraulic conductivity of unsaturated soils. Soil Sci Soc Am J 44: 892-898.
22. Mualem Y (1976) A new model for predicting the hydraulic conductivity of unsaturated porous media. Water Resour Res 12: 513-522.
23. Van Genuchten, M, Simunek F, Leij F, Sejna M (2009) The RETC code (version 6.02) for quantifying the hydraulic functions of unsaturated soils.
24. Mesinger F, Janjic Z (1974) Noise due to time-dependent boundary conditions in limited area models. The GARP Programme on Numerical Experimentation, Rep. No. 4, WMO, Geneva.
25. Black T (1994) The new NMC mesoscale Eta Model: Description and forecast examples. Weather Forecasting 9: 265-278.
26. Gellens D, Roulin E (1998) Streamflow response of Belgian Catchments to IPCC climate change scenarios. J Hydrol 210: 242-258.
27. Kroes J, Van Dam J, Groenendijk P, Hendriks R, Jacobs C (2008) SWAP version 3.2. Theory description and user manual. Wageningen, Alterra, Alterra Report 1649.

**Citation:** de Melo TM, Louzada JAS, Pedrollo OC (2014) Impacts of Climate Change on Soybean Irrigation Water Requirements in Northwest Region of Rio Grande do Sul, Brazil. Irrigat Drainage Sys Eng 3: 129. doi:10.4172/2168-9768.1000129